

Preparation of environmentally harmless paints based on self-crosslinking acrylate latexes and assessment their industrial coating properties

Denisa Steinerová*, Andréa Kalendová, and Jana Machotová

*Institute of Chemistry and Technology of Macromolecular Materials,
The University of Pardubice, CZ–532 10 Pardubice, Czech Republic*

This paper describes the properties of environmentally harmless anticorrosion paints based on newly synthesized water-based polymeric acrylate dispersions and containing magnesium oxide nanoparticles at a concentration of 1.5 % relative to the monomers. An aqueous dispersion obtained by the same procedure, i.e. semi-continuous emulsion polymerisation, but containing no MgO nanoparticles, had served as a reference system when evaluating the effect of the nanoparticles. The paints have been studied with respect to the effects of the new binder and of various environmentally harmless pigments possessing different chemical compositions and particle shapes on the anticorrosion efficiency of the paint film. The paint film's mechanical and chemical resistance was also evaluated because a high mechanical and chemical resistance of the coating is a prerequisite for high anticorrosion efficiency of the paint system. The results of measurements of the mechanical, chemical as well as corrosion resistance of the latex films have demonstrated better protective properties of the new polymeric dispersions with magnesium nanoparticles compared to the reference system that did not contain any nanoparticles.

Keywords: Ecological harmless paints; MgO nanoparticles; Anticorrosion protection

Introduction

Water-based paints are attracting interest in view of the ever-increasing pressure on environmental protection and industrial-product harmlessness; specifically, with a view to controlling atmospheric emissions of volatile organic compounds (VOC) [1–3]. Thus, latex-based paints are coming to the fore owing to their

* Corresponding author, ✉ steinerovadenisa@gmail.com

environmental friendliness and high technological level of their synthesis [4]. A conventional pathway of the formation of the latex films is primarily based on coalescence of polymeric particles [5], resulting from physical interconnection between the polymeric particles; the quality of coalescence being decisive for the final properties of the paint films. However, the properties of paint films obtained by physical crosslinking are inferior to those of the paint films obtained by chemical crosslinking [6]. Hence, it is appropriate to complete physical crosslinking with keto-hydrazide post-crosslinking (see Fig. 1), which is based on a reaction between the carbonyl groups included in the polymeric latex particles and the diamine moiety dissolved in the aqueous phase. Among the assets of this keto-hydrazide post-crosslinking are the facts that the process runs fast also at normal temperatures and the film also hardens fast (so, it can be used soon) and is fairly resistant to extreme temperatures [7–9].

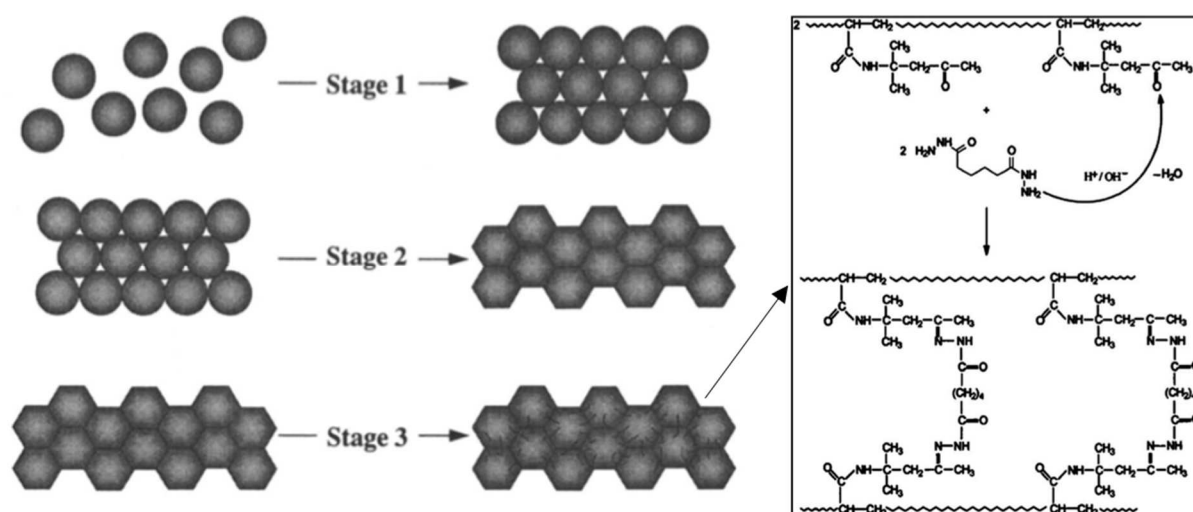


Fig. 1 Coalescence of latex film polymer particles (right) and keto-hydrazide post-crosslinking (left; taken from [10,11])

Latex paints have also some serious drawbacks – a lower anticorrosion resistance and an occurrence of flash corrosion, which is a phenomenon associated specifically with application of water-based paints on metallic substrates [12,13] and being due to soluble iron salts that penetrate into the paint film before the coalescence process is completed [5]. To reduce this effect, commercial paints contain the flash corrosion inhibitors (e.g. based on sodium nitrite), which, however, are considered harmful to human health [14]. Latex paints also exhibit a poorer chemical resistance and worse mechanical properties, i.e. features that are prerequisite for attaining a good anticorrosion efficiency of the paint system.

To counteract the drawbacks, magnesium oxide (MgO) nanoparticles were added to the system during the latex synthesis process. Magnesium oxide is toxicologically harmless and is not classified as a material endangering human

health or the environment [15–17]. Incorporation of the nanoparticles offers a new way of how to improve the use properties of the final paint film. In fact, MgO nanoparticles are partly water-soluble (MgO solubility in water at 30 °C is 8.6 mg in 100 mL), and the magnesium cations promote additional “ionic” (ionomeric) crosslinking during the reaction with the carboxyl groups bound to the polymeric chains. The approach consisting of the MgO nanoparticle addition during the synthesis was chosen for several reasons; among others, due to the alkaline environment of the latex (so-called “In Can” environmental protection), latex binder adhesion to the substrate (hydroxide ions formed), and uniform distribution of the magnesium nanoparticles in the aqueous phase between the particles of the copolymers present. In fact, nanoparticle powders require efficient dispersing during the mixing into the binder, which is a step that is, however, omitted here and so any industrial use of the dispersion will be simpler, etc.

The objective of the work presented here was to synthesize a new latex binder and develop environmentally harmless anticorrosion paints based on a self-crosslinking acrylate latex and nanostructural MgO that will exhibit good mechanical and chemical resistance, prevent flash corrosion and possess better anticorrosion properties than those of the reference acrylate polymeric dispersion without MgO nanoparticles.

Materials and methods

Synthesis and description of the acrylate dispersions

The water-based polymeric acrylate dispersions (latexes) were synthesized by using the following monomers: methyl methacrylate (MMA), *n*-butyl acrylate (BA), methacrylic acid (MAA) and diacetone acrylamide (DAAM), all from Sigma-Aldrich (St. Louis, MO, USA). Adipic dihydrazide – ADH (active substance content >98 %, Sigma-Aldrich) served as the crosslinking agent, Disponil FES 993 (anion-active surfactant based on fatty alcohol polyglycol ether sulphate, sodium salt) from BASF (Ludwigshafen, Germany) as the emulsifier, and ammonium peroxodisulphate (active substance content >99.9 %) from Lach-Ner, Neratovice, Czech Republic) as the initiator. Nanostructural MgO with no surface pretreatment, particle size <200 nm (commercial name: JR-NMg30) from Xuancheng Jingrui New Materials Co. (Hangzhouhangzhou, China) was added to the dispersions tested.

By semi-continuous emulsion polymerization technique were prepared two types of latexes: one with the added MgO nanoparticles as a part of the polymerization system (LM sample) and the other without nanoparticles (sample L0). The compositions of the polymers are specified in Tab. 1.

Table 1 The ratio of monomers and nanoparticles of latex dispersions

Sample	1. phase [g] MMA/BA/KMA	2. phase [g] MMA/BA/KMA/DAAM/MgO
LM	86/106/8	72/104/8/10/6
L0	86/106/8	72/104/8/10/0

Latexes were prepared according to the recipes listed in Tab. 2 in a glass reaction vessel at a polymerization temperature of 85 °C under an inert atmosphere of N₂. Distilled water, emulsifier and initiator were introduced into the reaction vessel before the dropwise addition of the monomer emulsion. The dropping was carried out in two phases. In the first one, the monomer emulsion was added dropwise for 60 min., followed by polymerization for 15 min. In the second phase, a monomer emulsion was added dropwise and MgO nanoparticles also added for the LM latex.

Table 2 Composition of the polymerization system

Reactor feed	[g]
Water	110.0
Disponil FES 993	1.0
Ammonium peroxodisulfate	30.8
1. phase	[g]
Water	120.0
Disponil FES 993	14.8
Ammonium peroxodisulfate	30.8
Monomers	200.0
2. phase	[g]
Water	220.0
Disponil FES 993	14.8
Ammonium peroxodisulfate	30.8
Monomers	200.0
Nanoparticles MgO	6.0

MgO nanoparticles were dispersed in acrylate monomers using a T18 digital ULTRA TURRAX disperser (IKA Works, Staufen, Germany) at 20,000 rpm for 30 min., followed by sonication in an ultrasonic bath (model KRAINTEK K-12.F, Kraitex, Podhájska, Slovakia) for another 30 min. Next, all the ingredients were mixed together and dispersed again for 3 min.

In this way, a monomer emulsion containing MgO nanoparticles was formed and dropped into the reaction vessel. After the addition was completed, the reaction system was allowed to polymerize for 120 min. After cooling, the latex without nanoparticles was adjusted to pH 8.5 with 10% aqueous ammonia. In the case of latex with nanoparticles, alkalization was not necessary since the latex pH was 10.34 due to the hydration of the nanostructured MgO. The self-crosslinked aqueous dispersions were obtained by mixing with 10% aqueous ADH in amounts matching the molar ratio DAAM : ADH = 2 : 1.

The coagulate/coarse impurity content was determined by sieve analysis (according to ČSN 64 9008). Non-Newtonian (apparent) viscosity was determined on a RotoVisco RT10/94 viscometer (HAAKE, Vreden, Germany) in the cone-plate arrangement of the Searle type (fixed bottom plate/movable rotor) at the following parameters: speed 0–250 rpm, slot width 0.05 mm, duration 180 s, temperature 21 °C. Temperature was held constant by using a Thermo Scientific Haake A10 temperature control unit (Thermo Fisher Scientific, Waltham, MA, USA), the minimum film-forming temperature was determined by using an MFFT-60 instrument (Rhopoint Instruments, East Sussex, UK) as per ISO 2115 and the real nanoparticle content of the coating film using inductively coupled plasma optical emission spectrometry (ICP-OES) on the instrument Thermo Scientific iCAP 7000 Series (Thermo Fisher Scientific). The non-volatile content was determined as per ČSN EN ISO 3251, pH was measured according to ČSN ISO 976 by using a Mettler Toledo FiveEasy FE20 pH-meter (Merck, Darmstadt, Germany), and binder density was measured pycnometrically as per ČSN EN ISO 2811-1 (Tab. 3).

Table 3 Basic properties of evaluated binders

Sample	Coagulate content [%]	Non-volatile content [%]	pH [–]	Apparent viscosity [mPa s]	Density [g cm ⁻³]	MFFT [°C]	Real nanoparticle content in film [%]
LM	2.98	42.58	10.34	90.86	1.0501	1.9	1.28
L0	0	40.98	8.44	30.97	1.0131	5.8	0

Pigments and fillers

The following commercially available anticorrosion pigments were used: calcium aluminium polyphosphosilicate (commercial name HEUCOPHOS® CAPP; role: chemically and electrochemically acting anticorrosion pigment; structure: mixture of aluminium phosphate $\text{Al}(\text{PO}_4)_3$ and calcium silicate CaSiO_3 ; pH 8.1, manufacturer/supplier: Heubach, Langelsheim, Germany), calcium magnesium phosphate (commercial name HEUCOPHOS® CMP; role: chemically and electrochemically acting anticorrosion pigment; structure: mixture of calcium

phosphate $\text{Ca}_3(\text{PO}_4)_2$ and magnesium phosphate $\text{Mg}_3(\text{PO}_4)_2$; pH 6.5, manufacturer/supplier: Heubach) and calcium hydrogen phosphate (commercial name HEUCOPHOS® CHP; role: chemically and electrochemically acting anticorrosion pigment; structure: anhydrous CaHPO_4 ; pH 7.6, manufacturer/supplier: Heubach). Pigments acting by the barrier mechanism were also used: wollastonite (commercial name Wollastonit K 1025; role: pigment acting by the barrier and chemical mechanisms; structure: the CaSiO_3 type with needle-shaped particles; pH 10.1, manufacturer/supplier: MINKO, Kutná Hora, Czech Republic), and talc (commercial name Mastek – Talc Naitsch SA-20; role: pigment acting by the barrier mechanism; structure: hydrated magnesium silicate of the $\text{Mg}_3\text{Si}_4\text{O}_{10}(\text{OH})_2$ type with lamellar particles; pH 7.0, manufacturer/supplier: Imerys Performance Additives, Paris, France). Hematite (commercial name Hematit Bayferrox 120 M; role: pigment for primers, structure: the $\alpha\text{-Fe}_2\text{O}_3$ type; pH 5–8, manufacturer/supplier: LANXESS, Cologne, Germany) and limestone (commercial name Omyacarb – 1VA; role: paint filler (pigment), structure: the CaCO_3 type; pH 9.0, manufacturer/supplier: Omya CZ, Lipová-lázně, Czech Republic) made the paints opaque.

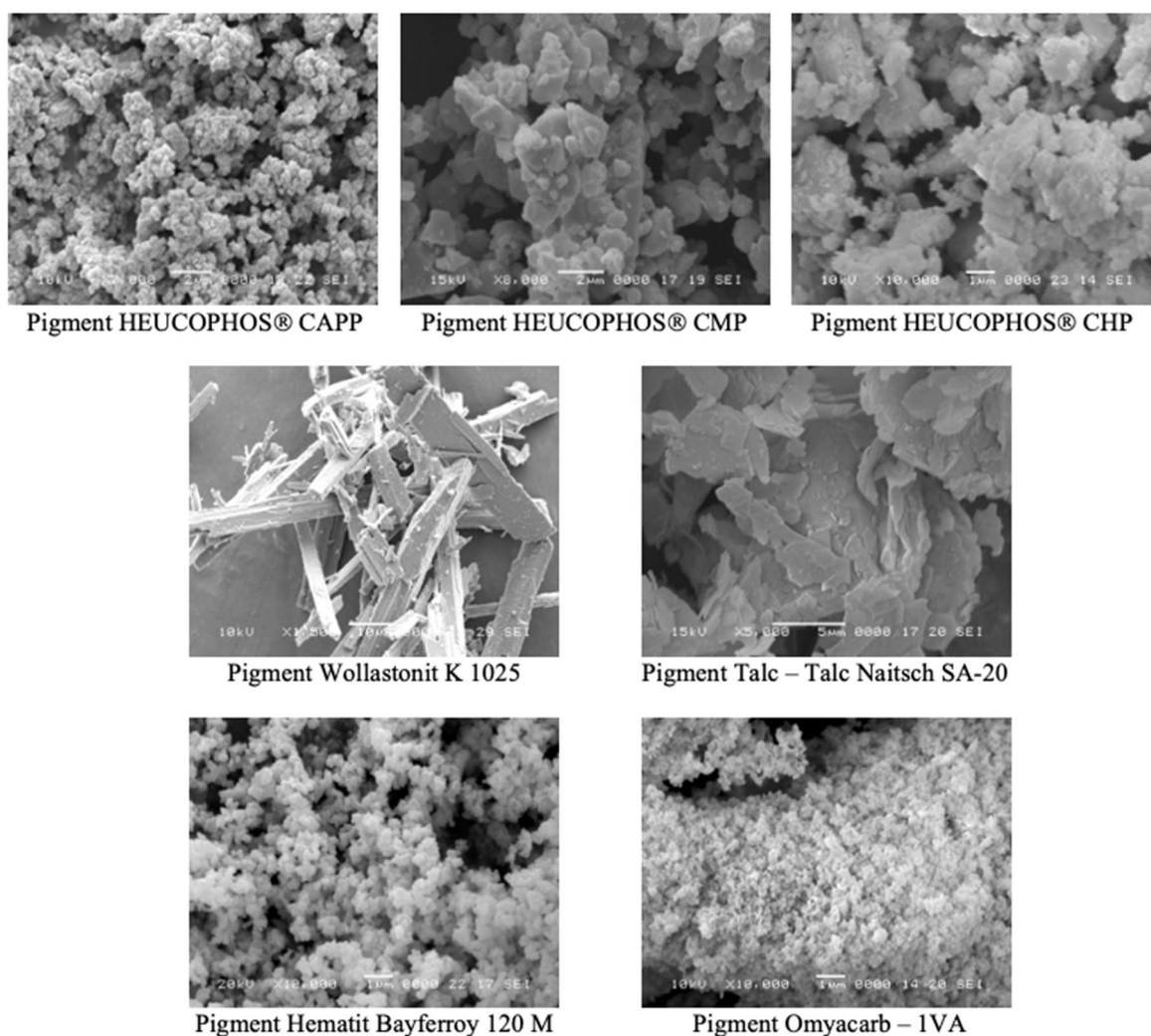


Fig. 2 Morphology of pigments and fillers used (SEM analysis)

Fig. 2 shows the morphology of the pigment and filler particles obtained by scanning electron microscopy (SEM) on a JSM-5600LV instrument (JEOL, Tokyo, Japan).

Formulation of the anticorrosion paints

First, the densities of the ingredients were measured on an AutoPycnometer 1320 helium pycnometer (Micrometritics, Norcross, GA, USA). Oil absorption was determined by the mortar-pestle method as per ČSN EN ISO 787-5 to obtain a figure required for calculation of the critical pigment volume concentration (CPVC). The size of the pigment particles, expressed as the diameter of an equivalent sphere [18] (i.e. sphere scattering laser radiation in the same manner as the particle in question), was measured on a MASTERSIZER 2000 instrument (Malvern Panalytical, Worcestershire, UK). The parameters of the pigments and fillers are surveyed in Tab. 4.

Table 4 Charakterization of pigments and fillers

Pigments*	Particle size d_{50} [μm]	Density [g cm^{-3}]	Oil absorption [g per 100 g_{PIG}]	CPVC [%]
P-CAPP	3.5	2.6018	44.58	44.51
P-CMP	2.8	2.7991	48.71	40.55
P-CHP	3.9	2.8773	39.73	44.85
P-T	10.5	2.8217	59.57	35.62
P-W	11.7	2.9042	32.71	49.46
P-H	0.27	5.0387	20.22	47.72
P-1VA	2.1	2.9350	23.84	57.07

* Abbreviations of anticorrosive pigments:

P-CAPP – HEUCOPHOS® CAPP, P-CMP – HEUCOPHOS® CMP, P-CHP – HEUCOPHOS® CHP, P-T – Talc Naitsch SA-20, P-W – Wollastonit K 1025, P-H – Hematit Bayferrox 120 M, P-1VA – Omyacarb – 1VA

The anticorrosion paints were prepared when applying a pigment volume concentration (PVC) of 5 %. The pigment Hematit Bayferrox 120 M was added in an amount increasing the PVC by 2 %, and the Omyacarb – 1VA was used to adjust the pigment system parameter to $Q = 50$ % ($Q = 100$ % means that $\text{PVC} = \text{CPVC}$; see Tab. 5). The systems were dispersed by using highly concentrated aqueous pigment pastes on a dissolver DISPERMAT CN from VMA-GETZMANN

(Reichshof, Germany). The following materials were added to the dispersing vessel to ensure desired dispersing and subsequent formation of a paint film free from any defects: NOPCOSPERSE N (sodium acrylate, manufacturer/supplier: Henkel, Düsseldorf, Germany) and Dispex® Ultra FA 4480 (monofunctional block copolymer of oleo alkylene oxide, active ingredient content >80%, manufacturer/supplier: BASF) as the dispersing additives; DEHYDRAN® (modified polysiloxanes, manufacturer/supplier: Henkel) as a defoamer; and BENTONE® EW ($\text{Na}_{(0.67)}(\text{Mg}, \text{Li})_6\text{Si}_8\text{O}_{20}(\text{OH}, \text{F})_4$ (smectite clay), purity >99%, manufacturer/supplier: Elementis, London, UK) as a rheological additive.

Table 5 Anticorrosion coating formulation

System		Binder [wt. %]	Pigment [wt. %]	P-H [wt. %]	P-IVA [wt. %]
Binder	Pigment				
LM	P-CAPP	63.84	4.66	3.88	27.63
	P-CHP	63.54	5.13	3.88	27.45
	P-CMP	64.18	5.03	3.89	26.89
	P-T	65.02	5.15	3.95	25.88
	P-W	63.07	5.15	3.85	27.94
L0	P-CAPP	65.12	4.51	3.74	26.63
	P-CHP	64.80	4.96	3.73	26.50
	P-CMP	65.41	4.78	3.73	25.93
	P-T	66.24	4.97	3.82	24.97
	P-W	64.31	4.98	3.70	27.01

Preparation of the paint films

The pigmented paints were applied to steel panels (Q-Panel steel Class 11 – ISO 3574 CR1; cold-rolled low-carbon steel) 215 mm × 45 mm × 1 mm size for the mechanical resistance tests, 102 mm × 51 mm × 0.8 mm for the flash corrosion tests; and 152 mm × 102 mm × 0.8 mm for the anticorrosion efficiency tests. Glass panels 200 mm × 100 mm × 5 mm size were used for the adhesion tests and chemical resistance tests. The panel surfaces were washed and/or degreased with chloroform before paint application. The paints were applied by using an applicator; i.e., a box ruler with precisely defined slot width (Bird type from Zehntner, Sissach, Switzerland). A slot width of 200 µm was used for the flash corrosion, chemical resistance and mechanical resistance tests. The corrosion tests were made on paint films consisting of three layers. The ruler slot width was 200 µm for the first layer and 250 µm for the second and third layers. Each layer had been allowed to dry for 48 hours before a next layer was applied, and the 3layer paint

film was finally allowed to dry for another 10 days in an air-conditioned room at 21 ± 2 °C and 55% RH (ČSN EN 23270). This approach was also applied to all the remaining samples (except those for the flash corrosion tests).

Evaluation of the anticorrosion paints

Mechanical resistance of the paint films was measured by the cupping test as per ČSN EN ISO 1520 on an Erichsen instrument (Elcometer, Manchester, UK). A cross cut had been made in the paint film and the value at which the paint layer detached from the substrate was measured. Resistance to bending was measured as per ČSN EN ISO 1519 on an Elcometer 1506 cylindrical mandrel bend tester (Elcometer) using a size 2 mandrel. Impact resistance was measured by the falling weight method (on obverse and reverse) as per ČSN EN ISO 6272 on an Elcometer 1615 variable impact tester (Elcometer). Adhesion was evaluated by the cross-cut test (ČSN ISO 2409) using a device with 1 mm knife spacing (Elcometer). Chemical resistance was assessed with respect to the effect of methyl ethyl ketone by the rub test (ASTM D-4752-10). Flash corrosion of the steel substrate was measured by the method described in ref. [19]: the coated steel panels were allowed to dry at 21 ± 2 °C and $50 \pm 5\%$ relative humidity for 2 hours and then stored in a refrigerator at 5 °C for 16 hours. Subsequently, the entire paint film area was covered with a sheet of filter paper wetted in distilled water and this system was additionally covered with a glass pane to achieve full contact between the paint film and water. In 2 hours of action at room temperature the filter paper was removed, the samples were dried, and the corrosion effects were evaluated on the ASTM D 610-85 scale (Fig. 3). In fact, such a scale is intended for the assessment of corrosion beneath coatings due to atmospheric corrosion, but it can also be applied with advantage to the assessment of the effects of flash corrosion [20].

Furthermore, the paint films were tested for corrosion resistance against wet atmospheres as per ČSN 03 8131 by 480-hour exposure in a condensation chamber (Kovofiniš, Ledec nad Sázavou, Czech Republic), and against neutral salt spray as per ČSN ISO 9227 by 360-hour exposure in an SKB400ATR salt-spray cabin (Liebisch, Bielefeld, Germany) when simulating environment with an enhanced chloride content. After assessing the corrosion effects on the paint film, the latter was removed with a paint remover and the corrosion effects on the steel panel were evaluated. The assessment was made by subjective methods and the results processed as laid down in applicable ASTM standards. The metal corrosion effects on the steel panel surface and on the paint film were assessed as per ASTM D 610-85, blistering on the paint film surface and in a test cut as per ASTM D 714-87, and, finally, corrosion in the test cut assessed as per ASTM D 1654-92. The data obtained were used to evaluate the paint film's anticorrosion efficiency as described in the respective norm (ČSN ISO 2409).

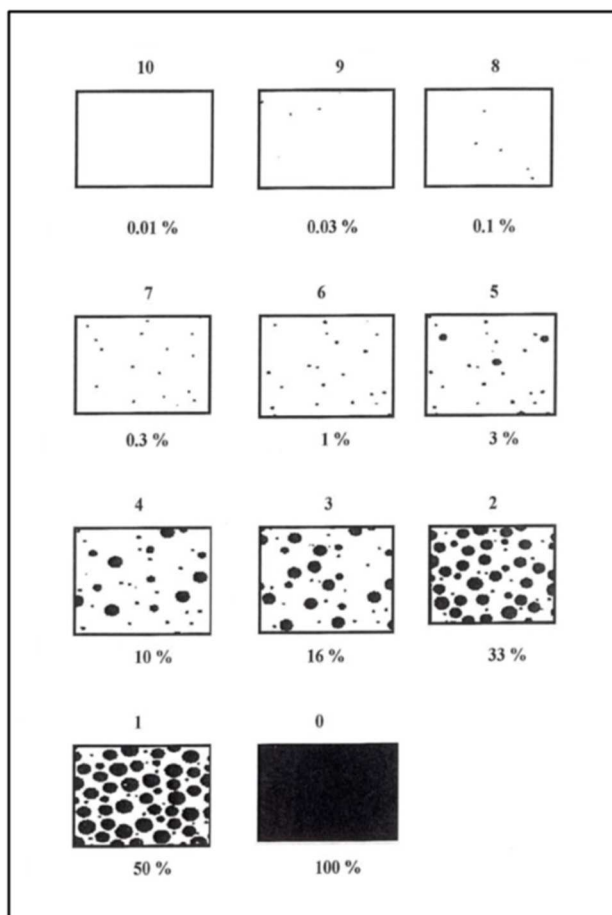


Fig. 3 Corrosion scale according to ASTM D 610-85 [20]

Results and discussion

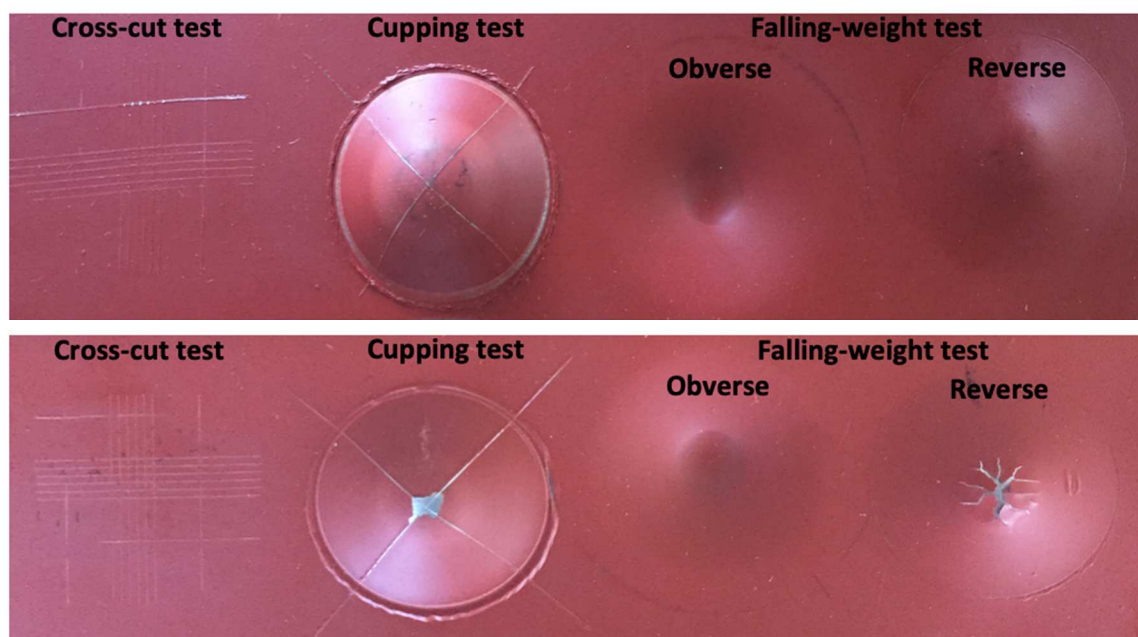
Mechanical properties

Mechanical resistance against deformation by external effects is among important properties of organic anticorrosion coatings. This property was evaluated on paint films $50 \pm 10 \mu\text{m}$ thick coated on steel panels. The following mechanical resistance tests were applied: (i) the cupping test, (ii) test by impact of a weight on the front and back sides of the coated panels, (iii) the bend test and (iv) the adhesion test for paint films on both glass and steel substrates. The paints based on the LM binder exhibited excellent mechanical resistance, superior to those observed for the paints based on the L0 binder (Tab. 6). Mechanical resistance of the former paints in the impact test on obverse and in the bend attained the maximum levels.

Table 6 Mechanical properties of coating films

System		Cupping test [mm]	Falling weight test – reverse [cm]	Cross-cut test [st.]	
Binder	Pigment			Glass	Metal
LM	P-CAPP	>10	>100	0	0
	P-CHP	>10	>100	0	0
	P-CMP	>10	>100	0	0
	P-T	>10	>100	0	0
	P-W	>10	>100	0	0
L0	P-CAPP	8.93	>100	1	0
	P-CHP	4.08	>100	1	0
	P-CMP	4.51	90	2	1
	P-T	>10	>100	1	0
	P-W	5.96	60	2	0

The superior mechanical resistance of the paints with LM (Fig. 4) is presumably due to the enhanced hydroplastification of the emulsion copolymers containing carboxyl groups owing to the OH^- ions present in the latex as a result of the reaction of the MgO nanoparticle surface with water. This brought about dissociation (ionisation) of the carboxyl groups, resulting in a higher elasticity. Among the paints based on L0, the highest mean mechanical resistance was observed for those containing talc (P-T) as the pigment; mainly, due to the lamellar shape of the talc particles.

**Fig. 4** Comparison of mechanical resistance of acrylate dispersions (top: LM, bottom: L0) with P-CAPP pigment

Chemical resistance

Resistance against methyl ethyl ketone was measured on paint films $40 \pm 10 \mu\text{m}$ thick deposited on glass panels. Once again, this resistance was substantially better for the paints based on LM containing nanoparticles MgO than those without nanoparticles MgO (L0), presumably due to the formation of ionic bonds between the magnesium cations (Mg^{2+}) and carboxy groups on the polymeric chains in systems containing nanoparticles. Only the paints containing calcium magnesium phosphate (P-CMP) exhibited a lower chemical resistance compared to the remaining pigments. This was observed for both types of latex (LM and L0) based paints (Fig. 5).

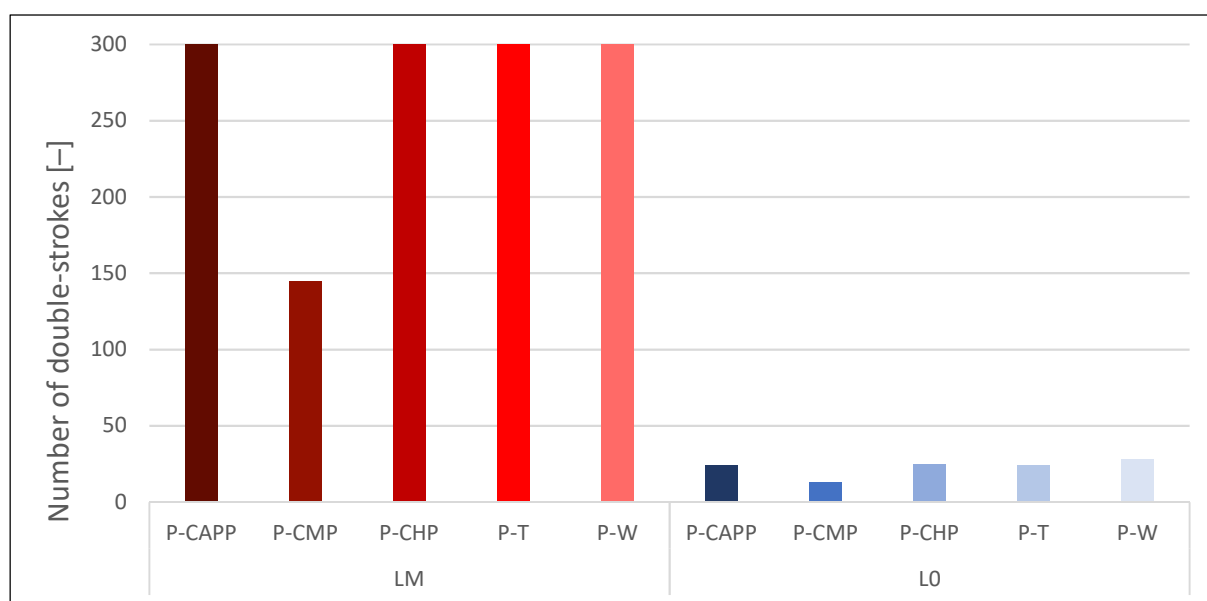


Fig. 5 Chemical resistance of coating films to methyl ethyl ketone

Flash corrosion

Flash corrosion of the steel substrate was observed only on panels without magnesium nanoparticles (L0). Hence, the MgO nanoparticles play the role of an efficient flash corrosion inhibitor, probably due to an alkaline action by dissolving a fraction of the MgO, resulting in a shift of the pH value near the steel to a region where metal corrosion is suppressed (Tab. 7); in fact, all the systems containing nanoparticles MgO (LM) having exhibited $\text{pH} > 10$ [21]. The pigments did not affect the resistance of latex with nanoparticle against flash corrosion appreciably. Among the paints without nanoparticles MgO (L0), those containing calcium aluminium polyphosphosilicate (P-CAPP) or calcium hydrogen phosphate (P-CHP) readings showed that the anticorrosion pigment had reduced the flash corrosion effects.

Table 7 Resistance of paint films to flash corrosion

System		Flash corrosion [%]	
Binder	Pigment	After 2 hours	Throughout the cycle
LM	P-CAPP	0.01	0.01
	P-CHP	0.01	0.01
	P-CMP	0.01	0.01
	P-T	0.01	0.01
	P-W	0.01	0.01
L0	P-CAPP	0.1	16
	P-CHP	0.03	16
	P-CMP	0.03	33
	P-T	0.1	33
	P-W	0.03	33

Corrosion resistance

Resistance of the anticorrosion paints against wet atmospheres was measured on paint films coated on steel panels at a thickness of $100 \pm 10 \mu\text{m}$ and provided with a test cut through the film down to the substrate. The panels were exposed to 100% RH air at $38 \pm 2 \text{ }^\circ\text{C}$ for 480 hours. No appreciable corrosion in the cut or metal corrosion effects on the paint surface was observed for any of the samples (Tab. 8). Each sample was inspected every 120 hours of exposure to the wet atmosphere: the samples containing nanoparticles MgO (LM) exhibited a rapid deterioration as early as the first 120 hours, remained constant during the subsequent period, whereas the samples without nanoparticles MgO (L0) exhibited corrosion effects increasing with time. Thus, the paints containing nanoparticles MgO (LM) can be expected to be more resistant during long-time exposure than the L0 based paints. The rapid deterioration of the samples containing nanoparticles MgO (LM) may have been due to the presence of interstitial areas containing residues of the emulsifier, initiator and, on top of that, some dissolved magnesium oxide, which altogether have constituted concentration cells causing blistering, and subsequently the reduced adhesion of the organic coating to the substrate. Water present in the coating induced corrosion effects and extraction of water-soluble substances. Once all the water-soluble substances have been washed out, no driving diffusion potential exists anymore and no additional corrosion effects take place. Neither type of latex showed significantly higher resistance against humid atmospheres due to the added effects of anticorrosion pigment.

Table 8 Resistance of the anticorrosion paints against wet after 480 hours exposure

System		Osmotic blisters of paint film	Rusting on surface paint film	Corrosion of metal substrate	Corrosion in cut	Osmotic blisters in cut
Binder	Pigment	[-]	[%]	[%]	[mm]	[-]
LM	P-CAPP	6MD	0.01	33	0	6M
	P-CHP	8M	1	16	0	8F
	P-CMP	8M	2	16	0	8F
	P-T	6M	3	10	0	8F
	P-W	6M	1	16	1.5	8F
L0	P-CAPP	4MD	1	33	0.2	8F
	P-CHP	6D	0.01	16	0	6M
	P-CMP	6MD	1	33	0.1	6M
	P-T	6MD	0.01	16	0.1	6MD
	P-W	6MD	3	33	0	6MD

The resistance of the anticorrosion paints to a neutral-salt spray atmosphere was measured on paint films coated on steel panels at a thickness of $100 \pm 10 \mu\text{m}$ and provided with a test cut through the film. The panels were exposed to the atmosphere containing 5 % NaCl spray at $35 \pm 1 \text{ }^\circ\text{C}$ for 360 hours.

Table 9 Resistance of the anticorrosion paints to a neutral salt spray atmosphere after 360 hours exposure

System		Osmotic blisters of paint film	Rusting on surface paint film	Corrosion of metal substrate	Corrosion in cut	Osmotic blisters in cut
Binder	Pigment	[-]	[%]	[%]	[mm]	[-]
LM	P-CAPP	6MD	0.01	16	0	8F
	P-CHP	6M	3	16	0.4	4MD
	P-CMP	6M	0.3	10	1	6MD
	P-T	4M	1	16	0	4MD
	P-W	4M	1	16	0.2	6MD
L0	P-CAPP	6MD	16	33	0	8F
	P-CHP	6D	33	33	0	6F
	P-CMP	6MD	16	50	0	8M
	P-T	4MD	16	50	0	6F
	P-W	6MD	33	50	0	6F

The results are listed in Tab. 9. Both systems exhibited the highest resistance if containing the calcium magnesium polyphosphosilicate (P-CAPP) based anticorrosion pigment. The paints containing nanoparticles MgO (LM) exhibited a higher resistance to the neutral-salt spray than those for all the monitored systems without nanoparticles MgO (L0) with the added appropriate anticorrosion pigment. This concerns particularly resistance of systems with nanoparticles MgO against corrosion of the steel substrate and corrosion effects appearing on the paint film surface (Fig. 6). Taking into account the results observed in the wet atmosphere test, it is suggested that here, also, corrosion resistance is reduced due to the presence of a high concentration of atmospheric water, bringing about extraction of water-soluble substances as outlined above.

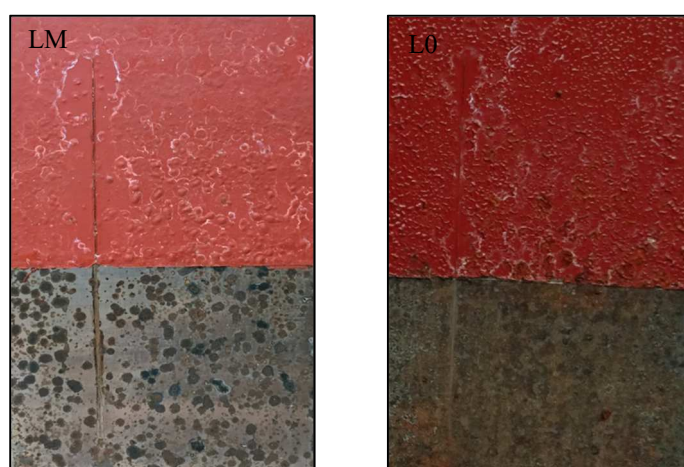


Fig. 6 Comparison of films resistance with P-CAPP pigment to neutral salt spray atmosphere after 360 hours exposure

Conclusion

This work has been devoted to the examination of environmentally harmless anticorrosion paint films based on water-dilutable self-crosslinking acrylate dispersions containing magnesium nanoparticles combined with environmentally harmless anticorrosion pigments possessing different chemical compositions and particle shapes with a view to identifying the best acting pigment for this system. The paint systems with the nanoparticles exhibited a high mechanical and chemical resistance, as well as resistance against flash corrosion of the steel substrate, much superior to the systems with no nanoparticles of MgO added. This was also true for the anticorrosion properties. Calcium aluminium polyphosphosilicate (P-CAPP) appeared to be the best pigment with respect to the corrosion inhibition properties of both paint systems. This may be due to its particle shape, suitable for the arrangement of the solid particles in the polymeric paint film, solubility, the actual pH and synergistic action with the Mg particles (in the case of binder with nanoparticles MgO).

Acknowledgment

The Technological Agency of the Czech Republic (TH02010140) is gratefully acknowledged for supporting this work.

References

- [1] Belis-Bergouignan M.-C., Oltra V., Saint Jean M.: Trajectories towards clean technology: Example of volatile organic compound emission reductions. *Ecological Economics* **48** (2004) 201–220.
- [2] Brown S. K., Sim M. R., Abramson M. J., Gray C.N.: Concentrations of volatile organic compounds in indoor air – A review. *Indoor Air* **4** (1994) 123–134.
- [3] Ramírez N., Cuadras A., Rovira E., Borrull F., Marcé R.M.: Chronic risk assessment of exposure to volatile organic compounds in the atmosphere near the largest Mediterranean industrial site. *Environment International* **39** (2012) 200–209.
- [4] Agrawal A. A., Konno K.: Latex: A Model for understanding mechanisms, ecology, and evolution of plant defense against herbivory. *Annual Review of Ecology, Evolution and Systematics* **40** (2009) 311–331.
- [5] Šňupárek J.: *Macromolecular chemistry: Introduction to polymer chemistry and technology* (in Czech). University of Pardubice, Pardubice 2014.
- [6] Rückerová A., Medunová M., Machotová J.: Crosslinking of waterborne coatings using a flame retardant (in Czech). *Chemické Listy* **112** (2018) 450–453.
- [7] Liu Y., Hou C., Jiao T., Song J., Zhang X., Xing R., Zhou J., Zhang L., Peng Q.: Self-assembled AgNP-containing nanocomposites constructed by electro-spinning as efficient dye photocatalyst materials for wastewater treatment. *Nanomaterials* **8** (2018) 1–14.
- [8] Machotová J., Rückerová A., Kalendová A., Pejchalová M.: *Waterborne self-crosslinking polymer dispersions with biocidal effect I* (in Czech). *Chemagazín* **10** (2017) 89–95.
- [9] Wang R.-M., Wang J.-F., Wang X.-W., He Y.-F., Zhu Y.-F., Jiang M.-L.: Preparation of acrylate-based copolymer emulsion and its humidity controlling mechanism in interior wall coatings. *Progress in Organic Coatings* **4** (2011) 369–375.
- [10] Eckersley S.T., Rudin A.: Film formation of acrylic copolymer latices: A model of stage II film formation, in: Provder T., Winnik M.A., Urban M.W. (Eds.): *Film formation in waterborne coatings*. American Chemical Society, Washington, DC 1996, pp. 2–21.
- [11] Zhang X., Liu Y., Huang H., Li Y., Chen H.: The diacetone acrylamide crosslinking reaction and its control of core-shell polyacrylate latices at ambient temperature. *Journal of Applied Polymer Science* **123** (2012) 1822–1832.
- [12] Novák P.: Types of metal corrosion (in Czech). *Koroze a ochrana materiálu* **49** (2005) 75–82.
- [13] Kalendová A.: Methods for testing and evaluating the flash corrosion. *Progress in Organic Coatings* **44** (2002) 201–209.

- [14] Kalendová A. (Ed.): *Antocorrosive pigments and paints: Conference proceedings* (in Czech). University of Pardubice, Pardubice 2002.
- [15] Di D.-R., He Z.-Z., Sun Z.-Q.: A new nano-cryosurgical modality for tumor treatment using biodegradable MgO nanoparticles. *Nanomedicine: Nanotechnology, Biology and Medicine* **8** (2012), 1233–1241.
- [16] Nguyen N.-Y.T., Grelling N., Wetteland C.L.: Antimicrobial activities and mechanisms of magnesium oxide nanoparticles (nMgO) against pathogenic bacteria, yeasts, and biofilms. *Scientific Reports* **8** (2018).
- [17] Jin T., He Y.: Antibacterial activities of magnesium oxide (MgO) nanoparticles against foodborne pathogens. *Journal of Nanoparticle Research* **13** (2011) 6877–6885.
- [18] Washington C.: *Particle size analysis in pharmaceuticals and other industries: Theory and practice*. E. Horwood, New York 1992.
- [19] Kalenda P., Veselý D., Antoš P.: *Corrosion and corrosion protection of metallic materials* (in Czech). University of Pardubice, Pardubice 2003.
- [20] Kalendová A.: *Methods for testing the properties of organic coatings: Part 1. Corrosion-inhibiting activity of organic coating* (in Czech). University of Pardubice, Pardubice 2001.
- [21] Zhang D.-Q., He X.-M., Cai Q.-R.: pH and iodide ion effect on corrosion inhibition of histidine self-assembled monolayer on copper. *Thin Solid Films* **518** (2010), 2745–2749.